

## Real-Time Monitoring of Catheter-Related Biofilm Infection in Mice

Xu Liu<sup>1†</sup>, Hong Yin<sup>2†</sup>, Xianxing Xu<sup>3</sup>, Yuanguo Cheng<sup>4</sup>, Yun Cai<sup>5\*</sup>, and Rui Wang<sup>5</sup>

<sup>1</sup>Department of Clinical Pharmacology, PLA General Hospital, Beijing 100853, P.R. China

<sup>2</sup>Traditional Chinese Medicine Pharmacy, PLA General Hospital, Beijing 100853, P.R. China

<sup>3</sup>Department of Pharmacy, the Second Artillery General Hospital, Beijing 100088, P.R. China

<sup>4</sup>State Key Laboratory of Pathogen and Biosecurity, Beijing Institute of Microbiology and Epidemiology, Beijing 100071, P.R. China

<sup>5</sup>Medicine Clinical Research Center, PLA General Hospital, Beijing 100853, P.R. China

Received: March 3, 2015

Revised: May 28, 2015

Accepted: June 2, 2015

First published online  
June 2, 2015

\*Corresponding author

Phone: +86-10-6693-7909;

Fax: +86-10-8821-4425;

E-mail: caicai\_hh@126.com

<sup>†</sup>These authors contributed  
equally to this work.

pISSN 1017-7825, eISSN 1738-8872

Copyright© 2015 by  
The Korean Society for Microbiology  
and Biotechnology

This study was done to establish a mouse model for catheter-related biofilm infection suitable to bioluminescence imaging (BLI). Biofilm formation of *Pseudomonas aeruginosa* (*P. aeruginosa*) Xen5 grown on catheter disks *in vitro* and in an implanted mouse model was real-time monitored during a 7-day study period using BLI. The numbers of integrated brightness (IB) and viable bacterial count (VBC) in the biofilm disks *in vitro* were highest at 24 h after inoculation; the IB of biofilm *in vivo* was increased until 24 h after implantation. A statistical correlation was observed between IB and VBC *in vitro* by linear regression analysis. The actual VBC value *in vivo* can be estimated accurately by IB without sacrifice. In addition, we monitored the change in white blood cells (WBCs) during infection. The number of WBCs on day 7 was significantly higher in the infection group than in the control group. This study indicates that BLI is a simple, fast, and sensitive method to measure catheter biofilm infection in mice.

**Keywords:** Bioluminescence imaging, biofilm, catheter-related infection, *in vivo*

### Introduction

A biofilm is a three-dimensional well-structured community of microorganisms encapsulated within a self-developed polymeric matrix that adheres irreversibly to host tissue or an implanted device [5]. The treatment of catheter-related biofilm infections is very difficult, because biofilm is highly tolerant to antimicrobial therapy and requires to replace infected foreign body material for cure [9]. To study catheter-related biofilm infections and evaluate the antimicrobial efficacy of antibiotics against biofilms, several animal models using subcutaneously implanted or vascular catheters have been successfully established. However, previous approaches could not achieve real-time monitoring of the biofilm and integrate both microbial and host contribution into the development of biofilm infections, but required the use of many animals [13, 15].

Bioluminescence imaging (BLI) is a new powerful method to analyze infectious diseases in animal models and microbial viability. It is characterized by high sensitivity,

ease of use, non-invasion, quantitative monitoring of infection, and less number of animals. Chauhan *et al.* [3] have developed a long-term biofilm infection model for some clinically relevant pathogens, such as *Escherichia coli*, *Pseudomonas aeruginosa* (*P. aeruginosa*), *Staphylococcus aureus*, and *Staphylococcus epidermidis*. They implanted a pediatric totally implantable venous access port with clinically relevant biofilms into adult rats and real-time monitored the biofilm development *in vivo* by using non-invasive and quantitative bioluminescence. Vande Velde *et al.* [16] demonstrated that it is feasible to monitor and quantitate *Candida albicans* biofilm formation from the yeast-to-hyphae state *in vitro* and *in vivo* by using a subcutaneous catheter rodent model for growth-phase-dependent bioluminescent *Candida albicans* strains. However, the experiments for monitoring the time-course of biofilm growth *in vitro* and *in vivo* and studying the statistical correlation between integrated brightness (IB) and viable bacterial count (VBC) have rarely been investigated.

Therefore, in the present study, we real-time monitored

biofilm development *in vitro* and *in vivo* using BLI and investigated the statistical correlation between IB and VBC. This study would contribute to a better understanding of catheter-related infections and provide a potential animal model to study biofilm therapies.

## Materials and Methods

### Biofilm Preparation and VBC Assay

*Pseudomonas aeruginosa* Xen5 (Caliper Life Science, PerkinElmer, Waltham, MA, USA) was derived from the parental strain *P. aeruginosa* ATCC 19660, a mucoid clinical strain isolated from human septicemia in Lima, Peru. *P. aeruginosa* Xen5 was engineered through conjugation and transposition of a plasmid carrying transposon Tn5 luxCDABE. *P. aeruginosa* Xen5 possesses a single stable copy of the *P. luminescens* lux operon on the bacterial chromosome. *P. aeruginosa* Xen5 biofilm was grown on catheter disks ( $r = 0.35$  cm). The catheter disks were placed into 24-well plates (one disk in each well) and cultured in 2 ml of Muller-Hinton (MH) Broth (BD Difco, Franklin Lakes, NJ, USA). Then 100  $\mu$ l of *P. aeruginosa* Xen5 suspension at 0.5 McFarland was inoculated into each well and cultured at 37°C for 6 h, and 1–7 d [14]. At each time point, six disks were randomly selected and rinsed with physiological saline to remove planktonic bacteria. The adherent bacteria were collected from disks by using an ultrasonic cleaning bath in 10 min. The bacteria solution was vigorously mixed and plated on MH agar plates at dilutions of  $10^{-1}$ ,  $10^{-2}$ ,  $10^{-3}$ ,  $10^{-4}$ , and  $10^{-5}$  for 16–24 h. The colony number on the plates was counted. The colony number between 30 and 300 per plate was considered an appropriate result, which was used for further experiments.

### *In Vivo* Biofilm Infected Model and Study Design

Experiments were approved by the Institutional Animal Care and Use Committee of Academy of Military Medical Sciences (No. AMMS-08-2014-001). Eighteen Kunming male mice, weighing 25–30 g, were acclimatized to a 12 h day/night cycle for 3 days prior to use and randomly assigned into two groups. All mice were intraperitoneally anesthetized with 0.01 ml/g 4% chloral hydrate. In the infection group ( $n = 9$ ), the disk from *P. aeruginosa* Xen5 inoculation for 1 day was rinsed with sterile physiological saline

solution and implanted at the dorsal midline as previously described [4], whereas in the control group, the bacteria-free disk was implanted into uninfected naive mice ( $n = 9$ ). After 7 days, the implanted disks in the two groups were taken out to examine the VBC of the biofilms.

### Bioluminescence Imaging of Biofilms

To develop biofilms *in vitro*, *P. aeruginosa* Xen5 was grown on catheter disks 24-well plates for 6 h, and 1–7 d. The process of infection was monitored daily to detect IB emission. The exposure time was about 30 sec. At each time point, six disks were randomly selected and transferred to a sterile plate (one disk per plate). The IB of bioluminescence was measured using a NightOWLIII 983 imaging system (Berthod Technologies, Bad Wildbad, Germany) and analyzed with IndoGO software (Caliper Life Science). The statistical correlation between VBC and IB was accessed by linear regression analysis [19]. To measure the IB *in vivo*, the mice in both groups were anesthetized using 4% chloral hydrate and then transferred into the machine to monitor. The color bar indicates the signal intensity, in which red and blue colors represent the high and low bioluminescent signals, respectively [2].

### Assay of WBCs, Rectal Temperature, and Body Weight

Blood (20  $\mu$ l) was drawn from the tail vein of each mouse before implanting and at 1, 3, 5, and 7 d after implanting. WBCs were examined using an animal blood analytical instrument (Mindray BC-2800Vet, Shenzhen, China). The data are presented as the mean  $\pm$  standard error of the mean (SEM) ( $n = 9$ ). The rectal temperature and body weight of all mice were measured every morning after implanting. The data are presented as the mean  $\pm$  standard deviation (SD) ( $n = 9$ ).

### Statistical Analysis

The linear regression for the statistical correlation between VBC and IB was performed, and  $R^2$  and two-tailed  $p$  values were reported.  $p < 0.05$  was considered statistically significant.

## Results

### *In Vitro* Biofilm Formation of *P. aeruginosa* Xen5 on Catheter

*P. aeruginosa* is one of the most frequently found

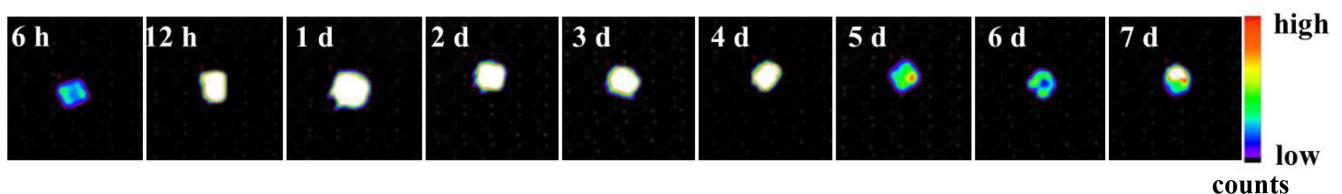


**Fig. 1.** Bioluminescence imaging (BLI) of *P. aeruginosa* Xen5 biofilm *in vitro*.

Biofilm formation of *P. aeruginosa* Xen5 on catheter disks was monitored by BLI at 6 h, 12 h, and 1–7 d at 37°C. Images were displayed in colors: red color represents the most intense light emission, while blue color corresponds to the weakest signal.

pathogens in catheterized patients. We chose it to establish a mouse model of biofilm infection. Biofilms of *P. aeruginosa* Xen5 were observed on catheter disks after inoculation for 6 h, 12 h, and 1–7 d at 37°C *in vitro*, which correlated with the results of BLI (Fig. 1). The signal strength in the images was highest on day 1. Therefore, according to the results of signal strength and VBC *in vitro*, catheter disks inoculated for 1 day were used for *in vivo* experiment.

#### *In Vivo* Biofilm Formation of *P. aeruginosa* Xen5 on Catheter

To investigate *in vivo* biofilm formation of *P. aeruginosa*, we implanted inoculated catheter disks into the dorsal midline of mice and monitored the IB of the biofilms every day. We observed that the bioluminescent signal was highest at 24 h after implanted, and the strength and area were gradually reduced with the prolongation of implantation. No signal was observed in the control group (Fig. 2A). Moreover, the rectal temperature in the infection group was significantly higher than that in the control group (Fig. 2B). The weight of control mice was slightly, but not significantly, higher than that of infected mice (Fig. 2C).

#### Statistical Correlation Between IB and VBC *In Vitro* and *In Vivo*

Real-time monitoring of the IB of biofilm development *in vitro* and *in vivo* was performed over a 7-day period, and the VBC of biofilms at 6 h, and 1–7 d was also examined. We found that the VBC was highest on day 1 (Fig. 3A). The IB of biofilm disks from the *in vitro* study strongly correlated with the VBC on these disks ( $Y = 0.750X + 1.648$ ,  $R^2 = 0.631$ ) (Fig. 3B). The VBC in the biofilm was examined on day 7. We found that the number of VBC in the infected catheter disks on day 7 of implantation was quite close to the estimated number according to the formula of linear regression from the *in vitro* study ( $p > 0.05$ ) (Fig. 3C).

#### Assay of WBCs

To verify the infection diagnosis, the number of WBCs was examined. The number of WBCs was gradually increased in the infection group in the 7-day study period, and in the control group only from day 0 to day 5 but restored to normal after day 5. There was no significant difference in the number of WBCs from day 0 to day 5 between the two groups, while the number of WBCs in the

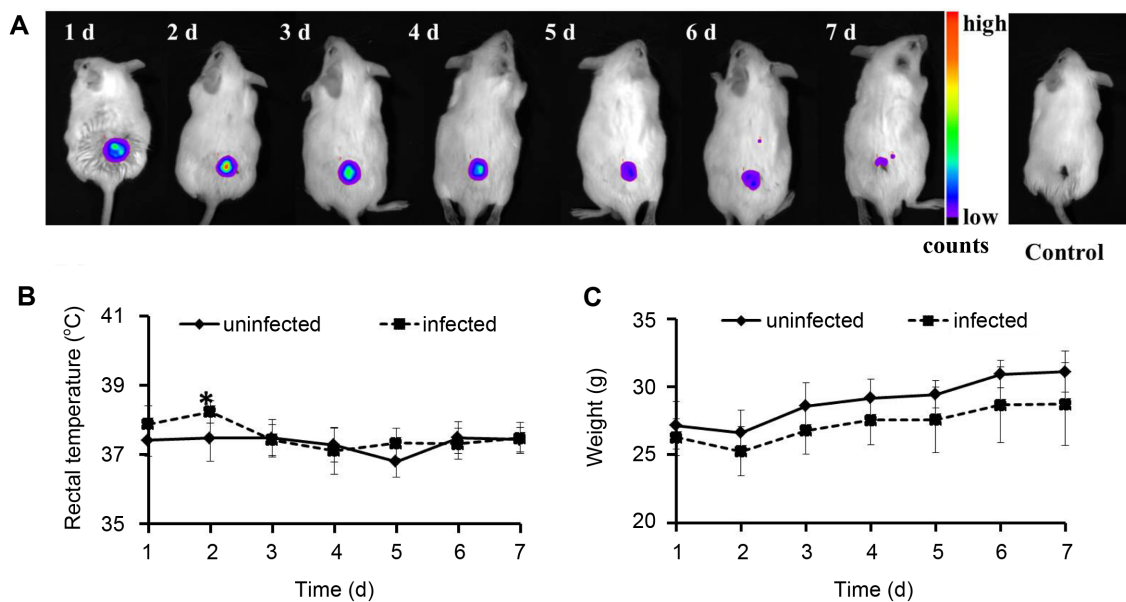


**Fig. 2.** Effects of *P. aeruginosa* Xen5 biofilm infections on rectal temperature and weight of mice.

(A) Real-time monitoring of *P. aeruginosa* Xen5 catheter biofilm infections in mouse model. Each mouse was implanted with one biofilm disk in the infected group. In the control group, uninfected naive mice were implanted with bacteria-free disks in the dorsal midline. We examined the bioluminescence signal over a 7-day period using a NightOWL II983 imaging system. As shown in the images, bioluminescence signals were observed in the dorsal midline region of mice. The color bar indicates the signal intensity, and red and blue colors represent high and low bioluminescent signals, respectively. (B) Measurement of the rectal temperature in mice ( $n = 9$ ) was conducted in the morning of 1–7 d. Change in temperature between the two groups was statistically different on day 2 after infection. \* $p < 0.05$ , uninfected group compared with infected group. (C) Measurement of mice weight ( $n = 9$ ) was conducted in the morning of 1–7 d.

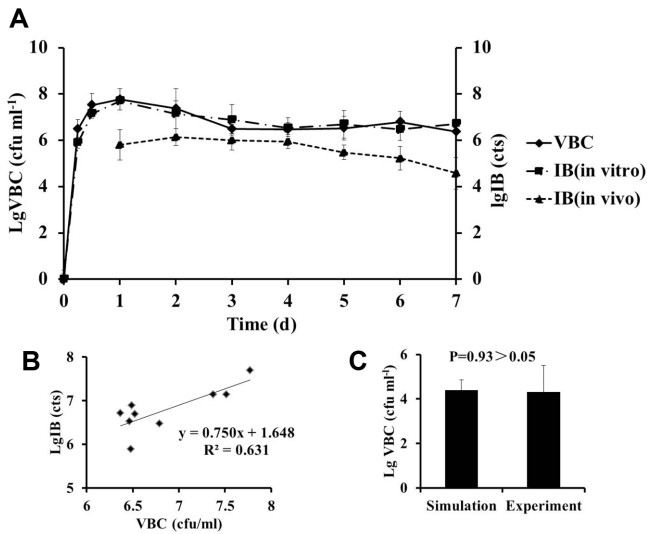


**Fig. 3.** Monitoring of *in vitro* and *in vivo* IB changes of *P. aeruginosa* Xen5 biofilms.

BLI showed a statistical correlation between IB and VBC *in vitro*, and IB could be used to calculate VBC *in vivo* by the liner regression formula without mice sacrifice. (A) Growth and bioluminescence curve of *P. aeruginosa* Xen5 biofilm development *in vitro* and *in vivo*. Each mouse was implanted with one disk with biofilm in the dorsal midline. Viable bacterial counts (VBC) of *P. aeruginosa* Xen5 biofilms were measured by agar plate counting at 0 h, 6 h, 12 h, 1–7 d and reported as CFU per ml. Bioluminescence was quantified as integrated brightness (IB) by using the NightOWL II983 imaging system and its software. Real-time bioluminescence monitoring of each catheter biofilm *in vitro* was performed at 0 h, 6 h, 12 h, 1–7 d and *in vivo* at 1–7 d. IB was compared with VBC at corresponding time points, and the data were presented as the mean ± standard deviation (SD) from six catheters *in vitro* and nine mice *in vivo*. (B) The statistical correlation between IB and VBC was analyzed by linear regression. (C) Monitoring of *P. aeruginosa* Xen5 catheter biofilm disks *in vivo* at 7 d after implantation was carried out by bioluminescence and agar plate counting. Simulation: catheter biofilm disks at 7 d *in vivo* was monitored by using bioluminescence and quantified as IB. VBC was calculated by the linear regression formula of IB and VBC *in vitro*,  $Y = 0.750X + 1.648$ .  $R^2 = 0.631$ . Experiment: catheter biofilm disks *in vivo* at 7 d were washed to remove planktonic bacteria, and VBC on biofilm disks was measured by agar plate counting. The results of simulation and experiment are presented as the mean ± SD ( $n = 9$ ).  $p = 0.93$ , simulation compared with experiment. The assay of IB and VBC was repeated three times for each mouse.

infection group was significantly higher on day 7 than that in the control group ( $p < 0.05$ ) (Fig. 4).

**Discussion**

Nowadays, it is still a big challenge in preventing and

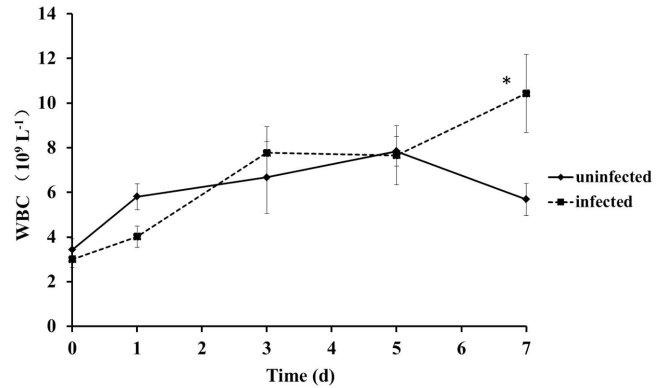


**Fig. 4.** Changes in WBCs in uninfected and infected mice. Data are presented as the mean ± standard error of the mean (SEM) ( $n = 9$ ). The assay of WBC was repeated three times for each mouse. WBC counts in two groups increased at 1 d and were statistically different at 7 d after infection.  $*p < 0.05$ , uninfected group compared with infected group.

treating biofilm-related infections owing to the lack of effective approaches. In animal models, low efficiency and high cost are the biggest issues in testing biofilm-related infections because it takes a long time to culture bacteria on agar plates and needs to sacrifice many animals to verify the results. BLI is a highly sensitive and quantitative method, and has been used for the rapid screening of bacteria in mice [16]. Here, we demonstrated that BLI can be used as a noninvasive approach to visualize and quantify the biofilm infection from *P. aeruginosa* Xen5.

Bioluminescent bacteria have previously been used as an infection model for *in vivo* study [1, 17]. In this study, we implanted catheter disks inoculated with *P. aeruginosa* Xen5 into normal mice and monitored the biofilm formation and change of WBCs. Here, we observed that the strength and area on the catheter disks in Fig. 1 were reduced but the VBC was stable *in vitro*. This observation confirmed that bioluminescence was specifically emitted from the infected catheter, and bacterial cells remain in the local region and did not cause systemic infection through the blood. Decreasing signals may be due to the decrease in bacterial activity and insufficient oxygen supply. Because luciferases are oxygenases, anaerobic environment may limit the use of BLI. A study reported that the bioluminescent signal of *Salmonella* in the abdominal region was greatly enhanced after air exposure [8]. Moreover, Hoiby *et al.* [10] revealed that the oxygen concentration is high on the surface of biofilms but low in the center of the biofilms. Thus, the anaerobic condition limits luciferases expression and bacterial activity [6]. The IB value of the biofilms from

day 1 of implantation was lower than that from *in vitro* inoculation on day 1. This difference may be caused by tissue absorption. Hemoglobin can absorb the blue and green part of the visible spectra, whereas red light can penetrate several centimeters of tissue [1]. *In vivo*, IB values continued to decrease from day 1 to the end of the study, but IB values from the *in vitro* study stabilized at the later stage of infection and were higher than those from the *in vivo* study over the post-infection period. We speculate that the immune system of mice may play a role in this point. To explore the feasibility that IB can reflect bacterial burden instead of VBC *in vivo*, we examined the statistical correlation between IB and VBC and observed a significant correlation *in vitro*. According to the formula of linear regression, we also found that the actual number of VBC in the infected catheter disks at day 7 of implantation was very close to the estimated number according to the formula of linear regression from the *in vitro* study. This result implies that the biofilm infection mice model is successful, and the host immune system is not able to clear biofilm infection, which supports the fact that catheter biofilm infections are latent and very difficult to clear *in vivo*. Therefore, in addition to VBC and electron microscopy, bioluminescence can accurately examine the level of bacterial colonization of the catheter biofilm disks and monitor the distribution and temporal patterns of biofilms without animal sacrifice.

The intensity and area of the biofilm signals were reduced in the *in vivo* imaging. The VBC on day 7 *in vivo* and the gradually increased WBCs suggest that the host immune system is not able to clear the biofilm, although it can control biofilm infection. Because WBCs showed significant difference on day 7 between *in vitro* and *in vivo*, it can be used as an infection model for long-time diagnosis, although the surgery might cause the risk of short-time infection to mice. The biological and physicochemical features of the biofilm structure protect the bacterium from environmental adversities and immune evasion, avoiding complement immunity and phagocytosis [18]. Bacteria within the biofilm produce endotoxins, which may in turn elicit immune responses. Disks with mature biofilm were planted in mice in a study, and biofilm barrier endotoxin release induced weaker host responses [7]. Thus the WBCs increased slightly in the early infection. As biofilm growth, detached individual bacteria from biofilm can obtain enough oxygen and nutrients growth rapidly [11, 12]. Without the prevention of biofilm, endotoxin released from planktonic bacteria would induce rapidly increase of WBCs. However, we need a rapid method to detect the early phase of

infection, like procalcitonin or C-reactive protein.

In conclusion, we have demonstrated that *P. aeruginosa* Xen5 can be visualized by noninvasive imaging in live mice during biofilm infection; this technique can be used to rapidly visualize and quantify biofilm infection. The model could be a fast and reliable method to evaluate the therapy efficacy for biofilm-related infections.

## Acknowledgments

Author contributions: Xu Liu, Hong Yin, Yun Cai, and Rui Wang contributed to the study design, experiments, and writing of this paper. Xianxing Xu and Yuanguo Cheng carried out the experiments.

This study was supported by grants from Beijing Natural Science Fund of China (No. 7122167), the Science Technological Innovation Nursery Fund of PLA General Hospital (No. 13KMM45), and the National Major Scientific and Technological Special Project for "Significant New Drugs Development" during the 12th Five-Year Plan Period (No. 2012ZX09303004-002).

## References

1. Andreu N, Zelmer A, Sampson SL, Ikeh M, Bancroft GJ, Schaible UE, et al. 2013. Rapid *in vivo* assessment of drug efficacy against *Mycobacterium tuberculosis* using an improved firefly luciferase. *J. Antimicrob. Chemother.* **68**: 2118-2127.
2. Bernthal NM, Stavrakis AI, Billi F, Cho JS, Kremen TJ, Simon SI, et al. 2010. A mouse model of post-arthroplasty *Staphylococcus aureus* joint infection to evaluate *in vivo* the efficacy of antimicrobial implant coatings. *PLoS One* **5**: e12580.
3. Chauhan A, Lebeaux D, Decante B, Kriegel I, Escande MC, Ghigo JM, Beloin C. 2012. A rat model of central venous catheter to study establishment of long-term bacterial biofilm and related acute and chronic infections. *PLoS One* **7**: e37281.
4. Chauhan A, Lebeaux D, Ghigo JM, Beloin C. 2012. Full and broad-spectrum *in vivo* eradication of catheter-associated biofilms using gentamicin-EDTA antibiotic lock therapy. *Antimicrob. Agents Chemother.* **56**: 6310-6318.
5. Cirioni O, Ghiselli R, Silvestri C, Minardi D, Gabrielli E, Orlando F, et al. 2011. Effect of the combination of clarithromycin and amikacin on *Pseudomonas aeruginosa* biofilm in an animal model of ureteral stent infection. *J. Antimicrob. Chemother.* **66**: 1318-1323.
6. Dinjaski N, Shalu S, Valle J, Lehman SM, Lasa I, Prieto MA, García AJ. 2014. Near-infrared fluorescence imaging as an alternative to bioluminescent bacteria to monitor biomaterial-associated infections. *Acta Biomater.* **10**: 2935-2944.



7. Donlan RM, Costerton JW. 2002. Biofilms: survival mechanisms of clinically relevant microorganisms. *Clin. Microbiol. Rev.* **15**: 167-193.
8. Foucault ML, Thomas L, Goussard S, Branchini BR, Grillot-Courvalin C. 2010. *In vivo* bioluminescence imaging for the study of intestinal colonization by *Escherichia coli* in mice. *Appl. Environ. Microbiol.* **76**: 264-274.
9. Fux CA, Wilson S, Stoodley P. 2004. Detachment characteristics and oxacillin resistance of *Staphylococcus aureus* biofilm emboli in an *in vitro* catheter infection model. *J. Bacteriol.* **186**: 4486-4491.
10. Hoiby N, Bjarnsholt T, Givskov M, Molin S, Ciofu O. 2010. Antibiotic resistance of bacterial biofilms. *Int. J. Antimicrob. Agents* **35**: 322-332.
11. Leid JG. 2009. Bacterial biofilms resist key host defenses. *Microbe* **4**: 66-70.
12. Lewis K. 2001. Riddle of biofilm resistance. *Antimicrob. Agents Chemother.* **45**: 999-1007.
13. Lu Q, Yu J, Bao L, Ran T, Zhong H. 2013. Effects of combined treatment with ambroxol and ciprofloxacin on catheter-associated *Pseudomonas aeruginosa* biofilms in a rat model. *Chemotherapy* **59**: 51-56.
14. Ochoa SA, López-Montiel F, Escalona G, Cruz-Córdova A, Dávila L, López-Martínez B. 2013. Pathogenic characteristics of *Pseudomonas aeruginosa* strains resistant to carbapenems associated with biofilm formation. *Bol. Med. Hosp. Infantil Mexico* **70**: 138-150.
15. Ozer M, Sinan H, Saydam M, Kilic A, Akyol M, Coskun A, et al. 2014. Effectiveness of *N*-butyl cyanoacrylate-based microbial skin sealant on the prevention of surgical site infections. *Surg. Infect. (Larchmt.)* **15**: 14-17.
16. Vande Velde G, Kucharikova S, Schrevens S, Himmelreich U, Van Dijck P. 2013. Towards non-invasive monitoring of pathogen-host interactions during *Candida albicans* biofilm formation using *in vivo* bioluminescence. *Cell Microbiol.* **16**: 115-130.
17. Vande Velde G, Kucharikova S, Van Dijck P, Himmelreich U. 2014. Bioluminescence imaging of fungal biofilm development in live animals. *Methods Mol. Biol.* **1098**: 153-167.
18. Vuong C, Kocianova S, Voyich JM, Yao Y, Fischer ER, DeLeo FR, Otto M. 2004. A crucial role for exopolysaccharide modification in bacterial biofilm formation, immune evasion, and virulence. *J. Biol. Chem.* **279**: 54881-54886.
19. Walton KD, Lord A, Kendall LV, Dow SW. 2014. Comparison of 3 real-time, quantitative murine models of staphylococcal biofilm infection by using *in vivo* bioluminescent imaging. *Comp. Med.* **64**: 25-33.